Bulgarian Chemical Communications, Volume 48, Number 4 (pp. 770– 778) 2016

An analysis of MHD natural convection heat and mass transfer flow with Hall effects of a heat absorbing, radiating and rotating fluid over an exponentially accelerated moving vertical plate with ramped temperature

G.S. Seth*, R. Tripathi, R. Sharma

Department of Applied Mathematics, Indian School of Mines, Dhanbad-826004, India

Received April 16, 2015; Revised December 16, 2015

An investigation of unsteady MHD natural convection heat and mass transfer flow with Hall effects and rotation of a viscous, incompressible, electrically conducting, radiating and temperature dependent heat absorbing fluid past an exponentially accelerated moving vertical plate with ramped temperature through a porous medium is carried out. An exact solution for fluid velocity fluid temperature and species concentration is obtained in a closed form by the Laplace transform technique. The expressions for shear stress, rate of heat transfer and rate of mass transfer at the plate are also derived. The numerical values of fluid velocity and fluid temperature are displayed graphically whereas those of shear stress and rate of heat transfer at the plate are presented in tabular form for various values of the pertinent flow parameters.

Keywords: Coriolis force, Hall current, Heat absorption, Ramped temperature and Thermal radiation

INTRODUCTION

The effects of thermal radiation and heat generation/absorption on hydromagnetic natural convection flow play a crucial role in controlling the heat transfer and may have promising applications in several physical problems of practical interest viz. convection in the earth's mantle, fire and combustion modeling, fluids undergoing exothermic and/or endothermic chemical reactions, building with buoyancy-driven natural ventilation, radiant ceiling heating systems and floor heating systems. Keeping in view the importance of such a study, Chamkha [1] studied the thermal radiation and buoyancy effects on hydromagnetic flow over an accelerating permeable surface with a heat source or sink. Seddeek [2] investigated the thermal radiation and buoyancy effects on MHD natural convection heat generating fluid flow past an accelerating permeable surface with a temperature-dependent viscosity. Ibrahim *et al*. [3] discussed the effects of radiation and absorption on the unsteady MHD free convection flow past a semi-infinite vertical permeable moving plate with chemical reaction and suction. Mohamed [4] considered chemical reactions and thermal radiation on hydromagnetic free convection flow with heat and mass transfer of a viscous fluid past a semi-infinite vertical moving porous plate embedded in a porous medium in the presence of thermal diffusion and heat generation. Prasad *et al.* [5] investigated the effects of internal heat generation/absorption, thermal radiation, magnetic field and temperature dependent thermal conductivity on the flow and heat transfer characteristics of a Non-Newtonian Maxwell fluid over a stretching sheet.

It is noticed that when the density of an electrically conducting fluid is low and/or the applied magnetic field is strong, Hall current plays a vital role in determining the flow-features of the fluid flow problems because it induces a secondary flow in the flow-field [6]. Taking this fact into account, Aboeldahab and Elbarbary [7] considered the effects of the Hall current on the magnetohydrodynamic free convection flow past a semi-infinite vertical plate with mass transfer. Saha *et al.* [8] discussed the effects of Hall current on the MHD laminar natural convection flow from a vertical permeable flat plate with a uniform surface temperature. Zueco *et al.* [9] made a numerical study of the unsteady MHD free convection flow with the mass transfer taking the Hall current and viscous dissipation into account. Ahmed *et al*. [10] considered the unsteady MHD free convective flow past a vertical porous plate immersed in a porous medium with Hall current, thermal diffusion and a heat source. It is noteworthy that the Hall current induces a secondary flow in the flow-field which is also the characteristics of Coriolis force. Therefore, it is essential to compare and contrast the effects of these two agencies and also to study their combined effects on such fluid flow problems. Considering these two effects, Takhar *et al*. [11] investigated the boundary layer flow of a viscous, incompressible and electrically conducting fluid over a moving surface in a rotating fluid, in the presence of a magnetic field and Hall current with a free moving stream. Recently, Seth *et al*. [12] considered the

* To whom all correspondence should be sent:
E-mail: gsseth_ism@yahoo.com; rajat17@am.ism.ac.in; rohitsharma@am.ism.ac.in

combined effects of the Hall current, rotation and radiation on natural convection heat and mass transfer flow past a moving vertical plate.

Natural convection flows are generally modeled by researchers under the consideration of uniform surface temperature or a uniform heat flux. However, practical problems often involve non-uniform thermal conditions. Some of the numerous industry based applications considering non-uniform thermal conditions include nuclear heat transfer control, materials processing, turbine blade heat transfer, electronic circuits and sealed gas-filled enclosure heat transfer operations. Keeping this fact in view, several researchers [13-23] investigated natural convection flow from a vertical plate with ramped temperature.

The current study seeks to investigate the effects of Hall current and rotation on unsteady hydromagnetic natural convection heat and mass transfer flow of a viscous, incompressible, electrically conducting, optically thin heat radiating and temperature dependent heat absorbing fluid through a fluid saturated porous medium past an exponentially accelerated vertical plate having the ramped temperature profile. This problem has not yet received attention from the researchers, although natural convection heat and mass transfer flow of a heat absorbing and radiating fluid resulting from such a ramped temperature profile of a plate moving with time dependent velocity may have strong bearings on numerous problems of practical interest where initial temperature profiles are of much significance in the design of hydromagnetic devices and in several industrial processes occurring at high temperatures where the effects of thermal radiation and heat absorption play a vital role in the fluid flow characteristics.

FORMULATION OF THE PROBLEM

Consider unsteady hydromagnetic natural convection flow of viscous, incompressible, electrically conducting, optically thin heat radiating and temperature dependent heat absorbing fluid past an infinite moving vertical plate embedded in a porous medium taking Hall current and rotation into account. The Cartesian co-ordinate system is considered in such a way that the $x'-$ axis is along the length of the plate in the upward direction and the $y'-$axis is normal to the plane of the plate in the fluid and the $z'-$ axis is perpendicular to the $x'y'-$ plane. The fluid is permeated by a uniform transverse magnetic field B_0 which is applied in a direction parallel to the y' axis. Initially i.e. at time $t' \le 0,$ both the fluid and plate are at rest and at a uniform temperature T'_∞. Also the species concentration within the fluid is maintained at a uniform concentration C'_∞. At time $t' > 0,$ the plate is exponentially accelerated with a velocity $U_0 e^{a't'}$ in the $x'-$direction and the temperature of the plate is raised or lowered to $T'_\infty + (T'_w - T'_\infty)t'/t_0$ when $t' \le t_0$ and thereafter at $t' > t_0,$ the plate is maintained at a uniform temperature T'_w. a' and U_0 are an arbitrary constant and uniform velocity of the plate (*i.e.* $a' = 0$) respectively. Also at time $t' > 0,$ the species concentration at the surface of the plate is raised to a uniform concentration C'_w and this is maintained thereafter. Since the plate is of infinite extent along the x' and z' directions and is electrically non-conducting, all the physical quantities depend only on y' and t'. The geometry of the problem is shown in Figure 1. It is assumed that the induced magnetic field produced by fluid motion is negligible in comparison to the applied one. This assumption is valid for metallic liquids and partially ionized fluids [24]. Also no electric field is applied so the effect of polarization of the fluid is neglected [25].

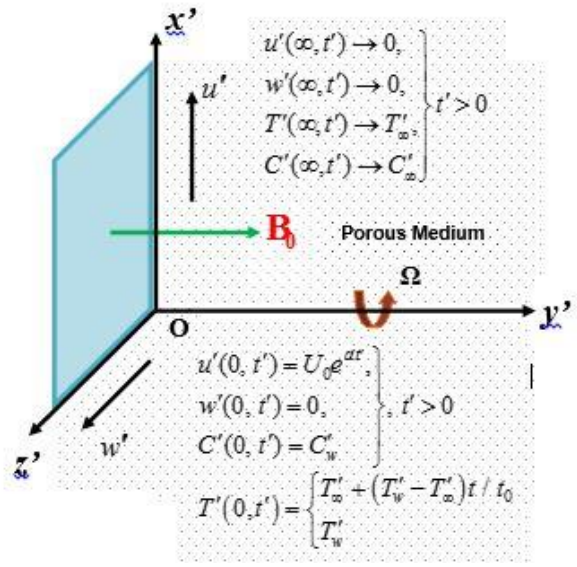

Fig.1. Geometry of the Problem

Keeping in view the assumptions made above, the governing equations for unsteady hydromagnetic natural convection flow of an electrically conducting, viscous, incompressible, temperature dependent heat absorbing and optically thin radiating fluid in a uniform porous medium, under Boussinesq's approximation, taking the Hall current and rotation into account are given by

$$\frac{\partial u'}{\partial t'} + 2\Omega w' = \nu \frac{\partial^2 u'}{\partial y'^2} - \left(\frac{\sigma B_0^{\,2}}{\rho}\right)\frac{(u' + mw')}{(1+m^2)} - \nu \frac{u'}{K_1'} + g\beta'(T' - T_\infty') + g\beta^*\left(C' - C_\infty'\right), \quad (1)$$

$$\frac{\partial w'}{\partial t'} - 2\Omega u' = \nu \frac{\partial^2 w'}{\partial y'^2} + \left(\frac{\sigma B_0^{\,2}}{\rho}\right)\frac{(mu' - w')}{(1+m^2)} - \nu \frac{w'}{K_1'}, \quad (2)$$

$$\frac{\partial T'}{\partial t'} = \frac{k}{\rho c_p}\frac{\partial^2 T'}{\partial y'^2} - \frac{Q_0}{\rho c_p}(T' - T_\infty') - \frac{1}{\rho c_p}\frac{\partial q_r'}{\partial y'}, \quad (3)$$

$$\frac{\partial C'}{\partial t'} = D_M \frac{\partial^2 C'}{\partial y'^2}, \quad (4)$$

where $m = \omega_e \tau_e$ is the Hall current parameter. $u', w', T', K_1', k, c_p, Q_0, C', D_M, q_r', \nu, \sigma, \rho, g, \beta', \beta^*$, ω_e and τ_e are, respectively, fluid velocity in the x'–direction, fluid velocity in the z'–direction, the fluid temperature, permeability of a porous medium, thermal conductivity, specific heat at constant pressure, heat absorption coefficient, species concentration, molecular (mass) diffusivity, radiating flux vector, kinematic coefficient of viscosity, electrical conductivity, fluid density, acceleration due to gravity, coefficient of thermal expansion, coefficient of expansion for species concentration, cyclotron frequency and the electron collision time.

The initial and boundary conditions for the fluid flow problem are

$$u' = w' = 0,\ T' = T_\infty',\ C' = C_\infty',\ \text{for } y' \geq 0 \text{ and } t' \leq 0, \quad (5a)$$

$$u' = U_0 e^{a't'},\ w' = 0,\ C' = C_w',\ \text{at } y' = 0 \text{ and } t > 0 \quad (5b)$$

$$T' = T_\infty' + (T_w' - T_\infty')t'/t_0,\ \text{at } y = 0 \text{ and } 0 < t' \leq t_0, \quad (5c)$$

$$T' = T_w',\ \text{at } y = 0 \text{ and } t' > t_0, \quad (5d)$$

$$u', w' \to 0, T' \to T_\infty', C' \to C_\infty', \text{as } y' \to \infty \text{ for } t' > 0 \quad (5e)$$

In the case of an optically thin gray fluid the local radiant absorption is expressed by

$$\frac{\partial q_r'}{\partial y'} = -4a^*\sigma^*\left(T_\infty'^4 - T'^4\right), \quad (6)$$

where a^* is the absorption coefficient and σ^* is the Stefan-Boltzmann constant.

Assuming a small temperature difference between the fluid temperature T' and the free stream temperature T_∞', T'^4 is expanded in a Taylor series about the free stream temperature T_∞' to linearize equation (6) which, after neglecting the second and higher order terms in $(T' - T_\infty')$, assumes the form

$$T'^4 \cong 4T_\infty'^3 T' - 3T_\infty'^4. \quad (7)$$

Making use of equations (6) and (7) in equation (3), we obtain

$$\frac{\partial T'}{\partial t'} = \frac{k}{\rho c_p}\frac{\partial^2 T'}{\partial y'^2} - \frac{16a^*\sigma^* T_\infty'^3}{\rho c_p}\left(T' - T_\infty'\right) - \frac{Q_0}{\rho c_p}\left(T' - T_\infty'\right). \quad (8)$$

In order to non-dimensionalize equations (1), (2), (4) and (8), the following non-dimensional variables and parameters are introduced

$$\left.\begin{aligned} &y = y'/U_0 t_0,\ u = u'/U_0,\ w = w'/U_0,\\ &t = t'/t_0,\ T = (T' - T_\infty')/(T_w' - T_\infty'),\\ &C = (C' - C_\infty')/(C_w' - C_\infty'), a = a'\nu/U_0^{\,2},\\ &G_r = g\beta'\nu(T_w' - T_\infty')/U_0^{\,3},\\ &G_c = g\beta^*\nu(C_w' - C_\infty')/U_0^{\,3},\\ &K^2 = \Omega\nu/U_0^{\,2}, K_1 = K_1' U_0^{\,2}/\nu^2,\\ &M = \sigma B_0^{\,2}\nu/\rho U_0^{\,2}, P_r = \nu\rho c_p/k,\\ &\phi = \nu Q_0/\rho c_p U_0^{\,2}, R = 16a^*\sigma\nu T_\infty'/U_0^{\,2}\rho c_p\\ &\text{and } S_c = \nu/D_M \end{aligned}\right\} \quad (9)$$

Equations (1), (2), (4) and (8), in non-dimensional form, are given by

$$\frac{\partial u}{\partial t} + 2K^2 w = \frac{\partial^2 u}{\partial y^2} - \frac{M(u + mw)}{(1+m^2)} - \frac{u}{K_1} + G_r T + G_c C, \quad (10)$$

$$\frac{\partial w}{\partial t} - 2K^2 u = \frac{\partial^2 w}{\partial y^2} + \frac{M(mu - w)}{(1+m^2)} - \frac{w}{K_1}, \quad (11)$$

$$\frac{\partial T}{\partial t} = \frac{1}{P_r}\frac{\partial^2 T}{\partial y^2} - RT - \phi T, \quad (12)$$

$$\frac{\partial C}{\partial t} = \frac{1}{S_c}\frac{\partial^2 C}{\partial y^2}, \quad (13)$$

where K^2, K_1, M, G_r, G_c, P_r, R, ϕ and S_c are, respectively, the rotation parameter, permeability parameter, magnetic parameter, thermal Grashof number, solution Grashof number, Prandtl number, radiation parameter, heat absorption parameter and Schmidt number.

It may be noted that the characteristic time t_0 is defined according to the non-dimensional process mentioned above, as

$$t_0 = \nu/U_0^{\,2}. \quad (14)$$

The initial and boundary conditions (5a) to (5e), in non-dimensional form, are given by

$$u = w = 0, T = 0, C = 0, \textbf{for} y \geq 0 \text{ and } t \leq 0, \quad (15a)$$

$$u = e^{at},\ w = 0,\ C = 1,\ \text{at } y = 0 \text{ and } t > 0, \quad (15b)$$

$$T = t,\ \text{at } y = 0 \text{ and } 0 < t \leq 1, \quad (15c)$$

$T=1$, at $y=0$ for $t>1$, (15d)

$u,\ w\to 0,\ T\to 0,\ C\to 0,$ as $y\to\infty$ for $t>0$, (15e)

where a is the plate acceleration parameter.

Combining equations (10) and (11), we obtain

$$\frac{\partial F}{\partial t}=\frac{\partial^2 F}{\partial y^2}-\left(N+\frac{1}{K_1}-2iK^2\right)F+G_rT+G_cC, \quad (16)$$

where $F=u+iw$ and $N=M/(1+im)$.

The initial and boundary conditions (15a) to (15e), in compact form, are given by

$F=0, T=0, C=0,$ for $y\geq 0$ and $t\leq 0$, (17a)

$F=e^{at},\ C=1,$ at $y=0$ for $t>0$, (17b)

$T=t,$ at $y=0$ for $0<t\leq 1$, (17c)

$T=1,$ at $y=0$ and $t>1$, (17d)

$F\to 0,\ T\to 0,\ C\to 0,$ as $y\to\infty$ for $t>0$. (17e)

Equations (12), (13) and (16) are subject to the initial and boundary conditions (17a) to (17e) and are solved by the Laplace transform technique. The exact solutions for the fluid temperature $T(y,t)$, species concentration $C(y,t)$ and fluid velocity $F(y,t)$ are obtained and presented in the following form after simplification

(i) For $\boldsymbol{P_r\neq 1}$ **and** $\boldsymbol{S_c\neq 1}$

$$T(y,t)=P(y,t)-H(t-1)P(y,t-1), \quad (18)$$

$$C=erfc\left(\frac{y\sqrt{S_c}}{2\sqrt{t}}\right), \quad (19)$$

$$F(y,t)=\left[\frac{e^{at}}{2}f_2(y,1,\beta_1,a,t)+\frac{\gamma}{2b_1}\left[e^{b_1t}\times\right.\right.$$
$$\left\{f_2(y,1,\beta_1,b_1,t)-f_2(y,S_c,0,b_1,t)\right\}-$$
$$\left.\left\{f_2(\mathrm{y},1,\beta_1,0,\mathrm{t})\right\}-f_2(\mathrm{y},\mathrm{S_c},0,0,\mathrm{t})\right\}\left.\right]\Big]$$
$$+G(y,t)+H(t-1)G(y,t-1). \quad (20)$$

(ii) For $\boldsymbol{P_r=S_c=1}$

$$T(y,t)=P_1(y,t)-H(t-1)P_1(y,t-1), \quad (21)$$

$$C(y,t)=erfc\left(\frac{y}{2\sqrt{t}}\right), \quad (22)$$

$$F(y,t)=\frac{e^{at}}{2}\left[f_2(y,1,\beta_1,a,t)\right]+\frac{b_2}{2}\left[f_2(y,1,0,0,t)\right.$$
$$\left.-f_2(y,1,\beta_1,0,t)\right]+G_1(y,t)-H(y,t-1)$$
$$\times G_1(y,t-1), \quad (23)$$

where

$P(y,t)=f_1(y,t,P_r,\beta_2)$,

$P_1(y,t)=f_1(y,t,1,\beta_2)$,

$$G(y,t)=\frac{\alpha}{2a_1^2}\left[e^{at}\left\{f_2(y,P_r,\beta_2,a_1,t)-\right.\right.$$
$$\left.-f_2(y,1,\beta_1,a_1,t)\right\}-a_1\left\{f_3(y,P_r,\beta_2,a_1,t)\right.$$
$$\left.\left.-f_3(y,1,\beta_2,a_1,t)\right\}\right],$$

$$G_1(y,t)=\frac{a_2}{2}\left[f_2(\mathrm{y},1,\beta_2,0,\mathrm{t})-f_1(y,t,1,\beta_1)\right],$$

$\beta_1=N+1/K_1-2iK^2,\ \beta_2=R+\phi,\ a_1=\dfrac{(P_r\beta_2-\beta_1)}{(1-P_r)}$,

$b_1=\beta_1/(S_c-1),\ \alpha=G_r/(1-P_r),\quad a_2=\dfrac{G_r}{\beta_1-\beta_2}$,

$b_2=\dfrac{G_c}{\beta_1}$ and $\gamma=G_c/(S_c-1)$.

$H(t-1)$ and $erfc(x)$ are, respectively, the unit step function and complementary error function. Expressions for f_1, f_2 and f_3 are provided in Appendix-I.

SHEAR STRESS AND RATE OF HEAT TRANSFER AT THE PLATE:

Expressions for the primary shear stress at the plate τ_x, secondary shear stress at the plate τ_z and rate of heat transfer at the plate N_u are obtained and presented in the following form after simplification

$$\tau=\tau_x+i\tau_z=e^{at}\left[f_4(\beta_1,1,a,t)\right]+\frac{\gamma}{b_1}\left\{f_4(\beta_1,1,b_1,t)\right.$$
$$\left.-f_4(0,S_c,b_1,t)\right\}-\left\{f_4(\beta_1,1,0,t)\right.$$
$$\left.-\frac{\sqrt{S_c}}{\sqrt{\pi t}}\right\}+G_2(0,t)+H(t-1)G_2(0,t-1), \quad (24)$$

$$N_u=P_2(0,t)-H(t-1)P_2(0,t-1), \quad (25)$$

where

$$G_2(0,t)=\frac{\alpha}{2a_1^2}\left[e^{a_1t}\left\{f_4(\beta_1,P_r,a_1,t)-f_4(\beta_1,1,a_1,t)\right\}\right.$$
$$\left.-a_1\left\{f_5(\beta_2,P_r,a_1,t)-f_5(\beta_1,1,a_1,t)\right\}\right],$$

$$P_2(0,t)=\left(\frac{1}{2}\right)\left[\left(2t\sqrt{P_r\beta_2}+\sqrt{\frac{P_r}{\beta_2}}\right)\left(erfc\left(\sqrt{\beta_2 t}\right)-1\right)\right.$$
$$\left.-2\sqrt{\frac{P_r}{t\pi}}e^{-\beta_2 t}\right].$$

The expressions for f_4 and f_5 are provided in Appendix-I.

Rate of mass transfer at the plate:

The expression for the rate of mass transfer at the plate S_h, is given by

$$S_h=-\sqrt{\frac{S_c}{t\pi}}. \quad (26)$$

Expression (26) reveals that rate of mass transfer at the plate increases on increasing the Schmidt number S_c and decreases on increasing the time. Since S_c presents a relative strength of the viscosity to molecular diffusivity of the fluid, S_c decreases on increasing the molecular diffusivity. This implies that the molecular diffusivity tends to reduce the rate of mass transfer at the plate and there is a reduction in rate of mass transfer at the plate with the progress of time.

RESULTS AND DISCUSSION

In order to analyze the physics of the flow regime, numerical computations from the analytical solutions (18) and (19) for the velocity field and temperature field and from the analytical expressions (24) and (25) for the shear stress and rate of heat transfer at the plate are carried out by assigning some chosen values to different physical parameters. Throughout our investigation, the values of the Prandtl number P_r, magnetic parameter M, permeability parameter K_1 and Schmidt number S_c have been fixed at 0.71, 15, 0.2 and 0.6 respectively as far as the numerical computations are concerned. It is known that $P_r = 0.71$ corresponds to the ionized air and $M = 15$ represents the strong magnetic field. The effects of the pertinent flow parameters on species concentration are already analyzed by Seth *et al.* [22]. Due to this reason, we have omitted the numerical computation for species concentration. The numerical results, computed from analytical solutions and expressions, are illustrated in Figures 2 to 12 along with Tables 1 to 5.

The variation of the primary velocity u and the secondary velocity w, versus the boundary layer co-ordinate y under the influence of the plate acceleration parameter a, Hall current parameter m, rotation parameter K^2, radiation parameter R, heat absorption parameter ϕ, thermal Grashof number G_r, solution Grashof number G_c and time t are depicted graphically in Figures 2 to 9. It is observed from these figures that the secondary velocity w attains a distinctive maximum value in the region near the plate and then decreases properly on increasing the boundary layer coordinate y to approach the free stream value. This may be due to the effects of the Coriolis force and Hall current which induce a secondary flow in the flow field.

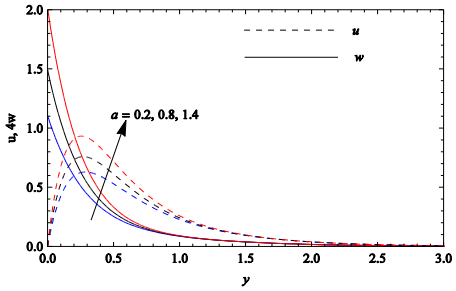

Fig. 2. Velocity profiles when $m = 0.5$, $K^2 = 2$, $R = 2, \phi = 3, G_r = 10, G_c = 3, S_c = 0.6$ and $t = 0.5$.

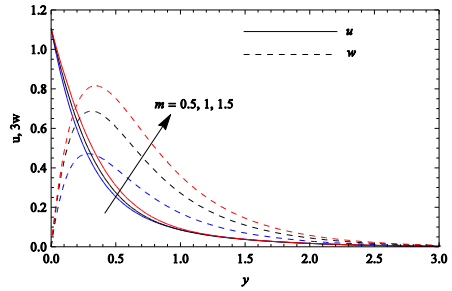

Fig. 3. Velocity profiles when $a = 0.2$, $K^2 = 2$, $R = 2, \phi = 3, G_r = 10, G_c = 3, S_c = 0.6$ and $t = 0.5$.

It is observed from Figure 2 that, an increase in the plate acceleration parameter a causes u and w to increase in the region near the plate and the effect of the plate acceleration parameter a is almost negligible in the region away from the plate. This observation suggests that the higher plate velocity results in an accelerated fluid motion in the region near the plate. It is inferred from Figure 3 that both u and w are getting accelerated on increasing m. This phenomena is in excellent agreement with the fact that in an electrically conducting fluid whose density is low and/or the applied magnetic field is strong, a current known as the Hall current is induced which moves in a direction normal to both the electric and magnetic field i.e. the total current produced in the flow-field does not move in the direction of the electric field. Thus, the Hall current has a tendency to accelerate both the primary and secondary fluid velocities. It is depicted from Figure 4 that, on increasing K^2, u gets decelerated whilst a reverse pattern occurs for w. This is in agreement with the fact that in a rotating medium, the Coriolis force (which is induced due to rotation) has a tendency to suppress the main flow i.e. the primary flow induces a secondary flow in the flow field. Figures 5 and 6 uniquely establish that there is a fall in the values of u and w for increasing values of R and ϕ. In other words, the primary and secondary velocities for highly radiating and heat absorbing fluids are smaller as compared to those of lesser radiating and heat absorbing fluids which is justified because the fluid temperature is getting reduced on

increasing R and ϕ which is clearly evident from Figures 10 and 11. It is inferred from Figures 7 and 8 that there is a significant increase in the values of u and w due to the increase in G_r and G_c. Since G_r presents the relative strength of the thermal buoyancy force to a viscous force and G_c is a measure of the solution buoyancy force to a viscous force, as G_r and G_c increase, the thermal and solutal buoyancy forces get stronger. This implies that the thermal as well as solution buoyancy forces tend to accelerate both the primary and secondary fluid velocities. It is revealed from Figure 9 that there is an increase in u and w on increasing t. This observation suggests that the primary and secondary fluid velocities are accelerated with the progress of time.

Figures 10 to 12 exhibit how the fluid temperature T is affected by the heat absorption parameter ϕ, radiation parameter R and time t. We see that, an increase in ϕ and R, results in a significant fall in the fluid temperature T. These results are in excellent agreement with the results of Nandkeolyar et al. [15] and Das et al. [20].

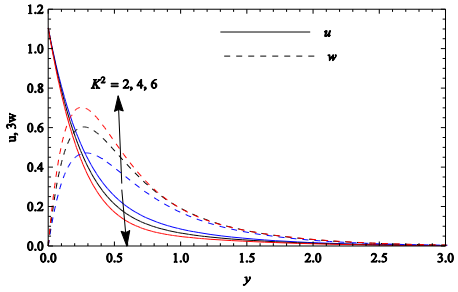

Fig. 4. Velocity profiles when $a = 0.2$, $m = 0.5$, $R = 2, \phi = 3, G_r = 10, G_c = 3, S_c = 0.6$ and $t = 0.5$.

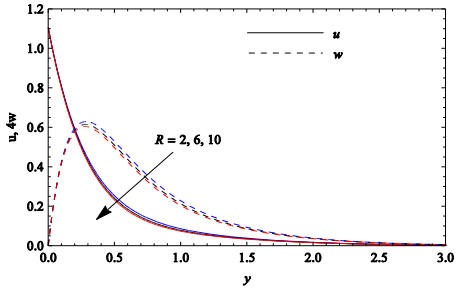

Fig 5. Velocity profiles when $a = 0.2$, $m = 0.5$, $K^2 = 2, \phi = 3, G_r = 10, G_c = 3, S_c = 0.6$ and $t = 0.5$.

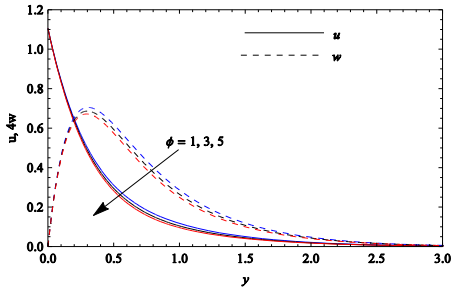

Fig. 6. Velocity profiles when $a = 0.2, m = 0.5$, $K^2 = 2$, $R = 2$, $G_r = 10$, $G_c = 3$, $S_c = 0.6$ and $t = 0.5$

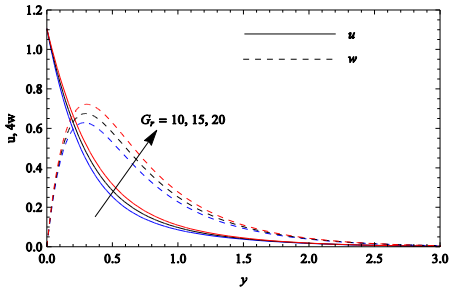

Fig. 7. Velocity profiles when $a = 0.2, m = 0.5$, $K^2 = 2$, $R = 2$, $\phi = 3$, , $G_c = 3$, $S_c = 0.6$ and $t = 0.5$

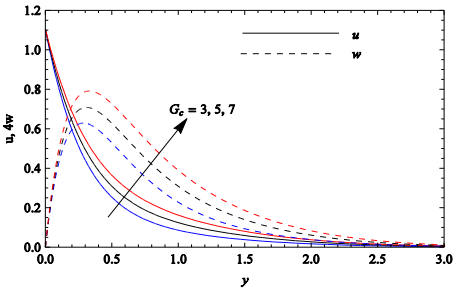

Fig. 8. Velocity profiles when $a = 0.2, m = 0.5$, $K^2 = 2$, $R = 2$, $\phi = 3$, $G_r = 10$, $S_c = 0.6$ and $t = 0.5$

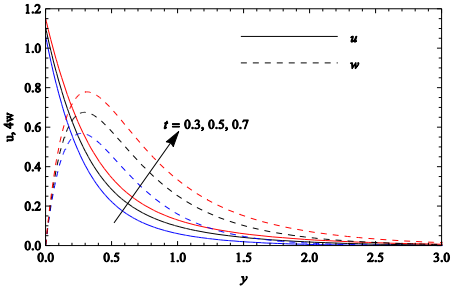

Fig. 9. Velocity profiles when $a = 0.2, m = 0.5$, $K^2 = 2$, $R = 2$, $\phi = 3$, $G_r = 10$, $G_c = 3$ and $S_c = 0.6$

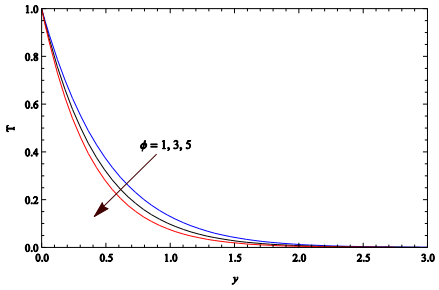

Fig. 10. Temperature profiles when $R = 2 \text{and} t = 0.5$

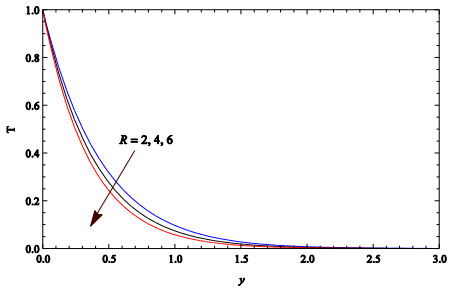

Fig. 11. Temperature profiles when $\phi = 3 \text{and} t = 0.5$

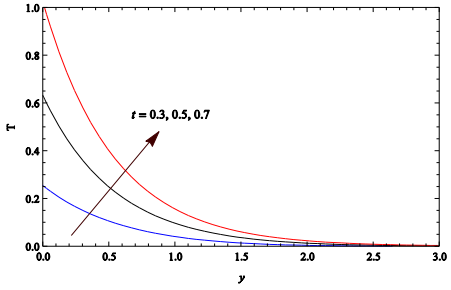

Fig. 12. Temperature profiles when $\phi = 3 \text{and} R = 2$.

The change in the behavior of the primary shear stress at the plate τ_x and secondary shear stress at the plate τ_z under the influence of K^2, m, G_r, G_c, ϕ, R, a and t, are presented in Tables 1 to 4. It is inferred from Table 1 that the primary shear stress at the plate τ_x increases on increasing K^2 and it decreases on increasing m. The secondary shear stress at the plate τ_z increases on increasing either K^2 or m.

This implies that the rotation tends to enhance the primary as well as secondary shear stress at the plate. The Hall current tends to reduce the primary shear stress at the plate whereas it has a reverse effect on the secondary shear stress at the plate. It is observed from Table 2 that τ_x decreases on increasing either G_c or G_r. τ_z increases on increasing either G_c or G_r. This implies that the thermal and solution buoyancy forces tend to reduce the primary shear stress at the plate whereas these agencies have a reverse effect on the secondary shear stress at the plate. It is evident from Table 3 that τ_x increases on increasing either ϕ or R whereas τ_z is decreased on increasing either ϕ or R. This implies that, heat absorption and radiation tend to enhance the primary shear stress at the plate whereas these agencies have a reverse effect on the secondary shear stress at the plate. It is clear from Table 4 that, τ_x and τ_z both increase on increasing a. τ_x decreases on increasing t whereas τ_z increases on increasing t.

Table 1. Shear stress at the plate when $G_r = 4$, $G_c = 3$, $\phi = 3$, $R = 2$, $S_c = 0.6$ and $t = 0.5$.

	$K^2 \downarrow$ $m \rightarrow$	0.5	1	1.5
$-\tau_x$	2	3.4336	2.8786	2.4015
	4	3.6436	3.1792	2.7645
	6	3.8789	3.4874	3.1401
τ_z	2	1.5472	2.0276	2.1685
	4	2.0784	2.5658	2.7408
	6	2.5528	3.0234	3.1977

Table 2. Shear stress at the plate when $m = 0.5$, $K^2 = 2$, $\phi = 3$, $R = 2$, $S_c = 0.6$ and $t = 0.5$

	$G_c \downarrow$ $G_r \rightarrow$	10	15	20
$-\tau_x$	3	3.4336	3.0806	2.7275
	5	3.0203	2.6673	2.3143
	7	2.6070	2.2540	1.9010
τ_z	3	1.6075	1.6836	1.7597
	5	1.7225	1.7986	1.8747
	7	1.8375	1.9136	1.9897

Table 3. Shear stress at the plate when $m = 0.5$, $K^2 = 2$, $G_r = 4$, $G_c = 3$, $S_c = 0.6$ and $t = 0.5$.

	$\phi \downarrow$ $R \rightarrow$	2	4	6
$-\tau_x$	1	3.3646	3.4336	3.4727
	3	3.4336	3.4727	3.4986
	5	3.4727	3.4986	3.5181
τ_z	1	1.5827	1.5472	1.5280
	3	1.5472	1.5280	1.5158
	5	1.5280	1.5158	1.5069

Table 4. Shear stress at the plate when $m = 0.5$, $K^2 = 2$, $G_r = 4$, $G_c = 3$, $\phi = 3$ **and** $R = 2$.

	$a \downarrow$ $t \rightarrow$	0.3	0.5	0.7
$-\tau_x$	0.2	3.5851	3.4336	3.3053
	0.4	3.8923	3.8605	3.7784
	0.6	4.2198	4.1456	4.0517
τ_z	0.2	1.4357	1.5472	1.6626
	0.4	1.5054	1.6750	1.8556
	0.6	1.5791	1.8157	2.0766

Table 5. Rate of heat transfer at the plate

R	ϕ	t	$-N_u$
		0.3	0.8845
2		0.5	1.1570
	3	0.7	1.5122
	1		1.0419
2	3	0.5	1.1570
	5		1.2838
2			1.1570
4	3	0.5	1.2838
6			1.4080

This implies that, both the primary and secondary shear stresses at the plate increase on accelerating the plate. Primary shear stress at the plate is getting reduced whereas secondary shear stress at the plate is getting enhanced with the progress of time. It is noticed from Table 5 that the rate of heat transfer N_u increases on increasing either of R, ϕ and t. This implies radiation and heat absorption tend to enhance the rate of heat transfer at the plate. The rate of heat transfer at the plate is getting enhanced with the progress of time.

CONCLUSION

The noteworthy results are summarized below

- Plate acceleration parameter, Hall current, thermal and solution buoyancy forces tend to accelerate the fluid flow in both the primary and secondary flow direction. Thermal radiation and heat absorption tend to decelerate the fluid flow in both the primary and secondary flow directions. Rotation tends to accelerate the primary fluid velocity whereas it has a reverse effect on the secondary fluid velocity. The primary and secondary fluid velocities get accelerated with the progress in time.
- Heat absorption and thermal radiation tend to reduce the fluid temperature. The fluid temperature is enhanced with the progress in time.
- Rotation, heat absorption, thermal radiation and the plate acceleration parameter tend to enhance the primary shear stress at the plate whereas the Hall current, thermal and solution buoyancy forces tend to reduce the primary shear stress at the plate. The rotation, Hall current, thermal and solution buoyancy forces and plate acceleration parameters tend to enhance the secondary shear stress at the plate whereas the heat absorption and thermal radiation tend to reduce the secondary shear stress at the plate. The primary shear stress at the plate is reduced, whereas the secondary shear stress at the plate is enhanced with the progress of time.
- The rate of heat transfer at the plate is enhanced on increasing either the heat absorption or thermal radiation with the progress of time.

Appendix

$$f_1(c_1,c_2,c_3,c_4)=\left(\frac{1}{2}\right)\left[\left(c_2+\frac{c_1}{2}\sqrt{\frac{c_3}{c_4}}\right)e^{c_1\sqrt{c_3c_4}}\right.$$
$$erfc\left(\frac{c_1}{2}\sqrt{\frac{c_3}{c_2}}+\sqrt{c_4c_2}\right)+\left(c_2-\frac{c_1}{2}\sqrt{\frac{c_3}{c_4}}\right)\times$$
$$\left.e^{-c_1\sqrt{c_3c_4}}erf\,c\left(\frac{c_1}{2}\sqrt{\frac{c_3}{c_2}}-\sqrt{c_4c_2}\right)\right],$$

$$f_2(c_1,c_2,c_3,c_4,c_5)=e^{c_1\sqrt{c_2(c_3+c_4)}}\,erfc\left(\frac{c_1}{2}\sqrt{\frac{c_2}{c_5}}\right.$$
$$\left.+\sqrt{(c_3+c_4)c_5}\right)-e^{-c_1\sqrt{c_2(c_3+c_4)}}\times$$

$$f_3(c_1,c_2,c_3,c_4,c_5)=\left(c_5+\frac{1}{c_4}+\frac{c_1}{2}\sqrt{\frac{c_2}{c_3}}\right)e^{c_1\sqrt{c_2c_3}}$$
$$\times erfc\left(\frac{c_1}{2}\sqrt{\frac{c_2}{c_5}}+\sqrt{c_3c_5}\right)+\left(c_5+\frac{1}{c_4}-\frac{c_1}{2}\sqrt{\frac{c_2}{c_3}}\right)e^{-c_1\sqrt{c_2c_3}}\times$$
$$erfc\left(\frac{c_1}{2}\sqrt{\frac{c_2}{c_5}}-\sqrt{c_3c_5}\right),$$
$$erfc\left(\frac{c_1}{2}\sqrt{\frac{c_2}{c_5}}-\sqrt{(c_3+c_4)c_5}\right),$$

$$f_4(c_1,c_2,c_3,c_4)=e^{-(c_1+c_3)c_4}\sqrt{\frac{c_2}{\pi t}}+\sqrt{(c_1+c_3)c_2}$$
$$\left\{erfc\left(\sqrt{(c_1+c_3)c_4}\right)-1\right\},$$

$$f_5(c_1,c_2,c_3,c_4)=2\left\{\sqrt{c_1c_2}\left(c_4+\frac{1}{c_3}\right)+\frac{1}{2}\sqrt{\frac{c_2}{c_1}}\times\right.$$
$$\left.\left\{erfc\left(\sqrt{c_1c_4}\right)\right\}-1\right\}$$

REFERENCES

1. A.J. Chamkha, *Int. J. Eng. Sci*., **38**, 1699 (2000).
2. M.A. Seddeek, *Canad. J. Phys.*, **79**, 725 (2001).
3. F.S. Ibrahim, A.M. Elaiw, A.A. Bakr, *Communications in Nonlinear Science and Numerical Simulation*, **13**, 1056 (2008).
4. R.A. Mohamed, *Appl. Math. Sci*., **3**, 629 (2009).
5. K. V. Prasad, K. Vajravelu, A. Sujatha, *J. Appl. Fluid Mech*., **6**, 249 (2013).
6. G.W. Sutton, A. Sherman, Engineering Magnetohydrodynamics Mcgraw-Hill, New York, 1965.
7. E.M. Aboeldahab, E.M.E. Elbarbary, *Int. J. Eng. Sci*., **39**, 1641 (2001).
8. L.K. Saha, M.A. Hossain, R.S.R. Gorla, *Int. J. Thermal Sci*., **46**, 790 (2007).
9. J. Zueco, P. Eguia, D. Patino, L.M. Lopez-Ochoa, *Int. J. Numer. Meth. Biomed. Engng*, **26**, 1687 (2010).
10. N. Ahmed, H. Kalita, D.P. Barua, *Int. J. Eng., Sci. Tech*., **2**, 59 (2010).

11. H.S. Takhar, A.J. Chamkha, G. Nath, *Int. J. Eng. Sci*., **40**, 1511 (2002).
12. G.S. Seth, S. Sarkar, S.M. Hussain, *Ain Shams Engineering Journal*, **5**, 489 (2014).
13. P. Chandran, N.C. Sacheti, A.K. Singh, *Heat Mass Transfer*, **41**, 459 (2005).
14. Samiulhaq, I. Khan, F. Ali, S. Shafie, *J. Phys. Soc. Jpn*, **81**, (2012), DOI: 10.1143/JPSJ.81.044401.
15. R. Nandkeolyar, M. Das, P. Sibanda, *Bound. Value Probl.*, **1**, 247 (2013).
16. A.Q. Mohamad, I. Khan, Z. Ismail, S. Shafie, *AIP Conf. Proc*., 1605, 398 (2014).
17. V. Rajesh, A.J. Chamkha, *Communications in Numerical Analysis*, **1,** 2014, (2014).
18. P.K. Kundu, K. Das, N. Acharya, *J.Mech.*, **30**, 277 (2014).
19. M. Das, B.K. Mahatha, R. Nandkeolyar, B.K. Mandal, K. Saurabh, *J. Appl. Fluid Mech*., **7**, 485 (2014).
20. S. Das, S.K. Guchhait, R.N. Jana, *J. Appl. Fluid Mech*., **7**, 683 (2014).
21. A. Khalid, I. Khan, S. Shafie, *Eur. Phys. J. Plus*, **57,** 130 (2015). DOI: 10.1140/epjp/i2015-15057-9.
22. G.S. Seth, S. Sarkar, S.M. Hussain, G.K. Mahato, *J. Appl. Fluid Mech*., **8**, 159 (2015).
23. G.S. Seth, S. Sarkar, *Bulg. Chem. Comm*., **47** (2015).
24. R. Cramer, S. I. Pai,Magnetofluid dynamics for engineers and applied physicts. McGraw Hill Book Company, New York. 1973
25. R.C. Meyer, *J. Aero. Science*, **25**, 561 (1958).

АНАЛИЗ НА ЕСТЕСТВЕНА КОНВЕКЦИЯ ПРИ МАГНИТО-ХИДРОДИНАМИЧЕН ПОТОК С ТОПЛО- И МАСОПРЕНАСЯНЕ С ЕФЕКТ НА ХОЛ ПРИ ОТНЕМАНЕ НА ТОПЛИНА И ИЗЛЪЧВАНЕ В РОТИРАЩ ФЛУИД НАД ЕКСПОНЕНЦИАЛНО УСКОРЯВАНА ПОДВИЖНА ПЛОСКОСТ С НЕРАВНОМЕРНО НАГРЯВАНЕ

Г.С. Сетх*, Р. Трипатхи, Р. Шарма

Департамент по приложна математика, Индийско училище по минно дело, Дханбад, Индия

Постъпила на 16 април, 2015 г.; коригирана на 16 декември, 2015 г.

(Резюме)

Изследвана е нестационарната естествена конвекция при магнитно-хидродинамичен поток с ефект на Хол, придружен с топло- и масопренасяне. Основното течение е ротационно, а флуидът е вискозен, несвиваем, електропроводящ и излъчващ. Течението е в близост до плоска, ускоряваща се стена с неравномерно разпределение на температурата. Точно решение в затворена форма за разпределението на температурата е намерено с помощта на Лапласова трансформация. Изведени са зависимости за срязващото напрежение, скоростта на топлопренасяне и скоростта на масопренасяне от плоскостта. Числените стойности на скоростта на флуида и на температурата са представени графично, докато тези са срязващото напрежение и скоростта на топлопренасяне са в таблична форма за различни управляващи параметри.